# Dielectronic recombination coefficients for fluorinelike ions: The multiconfiguration Dirac-Fock calculations

Mau Hsiung Chen
*High Temperature Physics Division, Lawrence Livermore National Laboratory, University of California, Livermore, California 94550*
(Received 30 March 1988)

Dielectronic recombination rate coefficients for the three initial states of the F-like ions have been calculated for six ions with $Z=26$, 35, 42, 47, 54, and 63. The calculations were carried out in the isolated resonance approximation for temperatures in the range $0.01 \leq T \leq 9$ keV. The Auger and radiation rates for each autoionizing state were computed explicitly by use of the multiconfiguration Dirac-Fock model in intermediate coupling with configuration interaction. Comparison is made with previous calculations. The effect of relativity on the Coster-Kronig-type transitions is also discussed.

## I. INTRODUCTION

Dielectronic recombination (DR) is one of the most important recombination processes for high-temperature plasmas produced in the laboratory or in astrophysics.[1-3] Knowledge of DR rate coefficients is essential in the determination of the ionization balance[4] and the plasma kinetics.[5] In the earlier modeling of the high-temperature plasmas the DR process is often represented by the semiempirical analytic rate coefficients.[1,6] Recently, many *ab initio* calculations have been carried out to determine the DR rate coefficients.[7-13] The DR rate coefficients for the F-like ions have been calculated by Roszman using nonrelativistic Hartree-Fock model.[14] There exist two other relativistic calculations[15,16] dealing with the DR rate coefficients for the F-like selenium.

In this paper we report on a systematic study of dielectronic-recombination rate coefficients for the three initial states of the F-like ions. The calculations cover six ions with atomic number $Z=26$, 35, 42, 47, 54, and 63. The detailed Auger and radiative rates for numerous intermediate autoionizing states were evaluated using the multiconfiguration Dirac-Fock model (MCDF).[7,17,18]

## II. THEORETICAL METHOD

In the isolated resonance approximation, the dielectronic-recombination coefficient from an initial state $i$ to a final state $f$ via an intermediate state $d$ after averaging over the Maxwellian distribution of the plasma electrons can be written as[2]

$$\alpha_{\mathrm{DR}}(idf)=\frac{1}{2g_i}\left[\frac{4\pi R}{kT}\right]^{3/2} a_0^3 \exp(-e_2/kT) \times g_d A_a(d\rightarrow i)\omega_d \ , \tag{1}$$

with

$$\omega_d = A_r(d\rightarrow f)/[\Gamma_r(d)+\Gamma_a(d)] \ . \tag{2}$$

Here $g_d$ and $g_i$ are the statistical weight factors; $R$ is the Rydberg energy and $a_0$ is the Bohr radius; $A_a(d-i)$ is the Auger rate and $A_r(d-f)$ is the radiative rate; $e_2$ is the Auger energy and $T$ is the electron temperature; and $\Gamma_r$ and $\Gamma_a$ are the total radiative and Auger rates, respectively. The total dielectronic-recombination rate coefficient can be obtained from Eq. (1) by summing over the intermediate autoionizing states $d$ and the final radiative stabilized states $f$.

In the present work, the decay rates and transition energies required in the evaluation of Eqs. (1) and (2) were calculated explicitly for each autoionizing state. From perturbation theory, the Auger transition probability in a frozen-orbital approximation is given by[17,19]

$$A_d(d\rightarrow i)=\frac{2\pi}{\hbar}\left|\left\langle \Psi_i \left| \sum_{\substack{\alpha,\beta \\ (\alpha<\beta)}} V_{\alpha\beta} \right| \Psi_d \right\rangle\right|^2 \rho(\varepsilon) \ . \tag{3}$$

Here $\rho(\varepsilon)$ is the density of final states and the two-electron operator $V_{\alpha\beta}$ is taken to be the Coulomb operator.

The spontaneous electric-dipole radiative transition probability for a discrete transition $d\rightarrow f$ is given in perturbation theory by[20]

$$A_r(d\rightarrow f)=\frac{2\pi}{3(2J_d+1)} |\langle f\|T_1\|d\rangle|^2 \ , \tag{4}$$

where $\langle f\|T_1\|d\rangle$ is the electric-dipole reduced matrix element.[20]

In the present work, the transition matrix elements in Eqs. (3) and (4) were evaluated in the framework of the MCDF model. For detailed derivation, the reader is referred to Ref. 17.

## III. NUMERICAL CALCULATIONS

Dielectronic recombination from a state of a F-like ion to a state of a Ne-like ion can be represented by

$$\begin{aligned}(2s^2 2p^5+2s2p^6)+e \rightleftarrows & (2s^2 2p^4 nln'l'+2s2p^5 nln'l' \\ & +2s^0 2p^6 nln'l') \\ \rightarrow & (2s^2 2p^5 n''l''+2s2p^6 n''l'')+h\nu \ ,\end{aligned} \tag{5}$$

and

$$2s^2 2p^5 + e \rightleftarrows 2s 2p^6 n_1 l_1 \rightarrow (2s^2 2p^5 n_1 l_1 + 2s 2p^6 n_2 l_2 + 2s^2 2p^6) + h\nu \ . \quad (6)$$

For the $\Delta n \neq 0$ transitions [Eq. (5)], we include the contributions from the doubly excited configurations with $n=3$, $l=0-2$ and $n' \geq 3$, $l' \leq 5$. For certain large $n'$, the Auger transitions to the Ne-like excited states become energetically possible. These transitions were also taken into account in calculations of the fluorescence yield $\omega_d$ [Eq. (2)]. In the case of Coster-Kronig capture ($\Delta n=0$) [Eq. (6)], the onset of the Coster-Kronig transition at $n_1 = n_0$ is determined by the MCDF calculations for each specific ion. For the Coster-Kronig transitions, we include the contributions from the autoionizing states with $n_1 \geq n_0$ and $l_1 \leq 8$. All the radiative transitions to the bound states were taken into account. The radiative transitions among the autoionizing states, however, were neglected in the present calculations.

The atomic energy levels and bound-state wave functions were calculated using the MCDF model in the average-level scheme.[18] The calculations were carried out in intermediate coupling with configuration interaction from the same complex. Explicit calculations were performed for the Auger-type [Eq. (5)] and Coster-Kronig–type [Eq. (6)] transitions up to $n'=10$ and $n_1=20$, respectively. The contributions from the autoionizing levels with $10 < n' \leq 30$ for the $\Delta n \neq 0$ transitions and $20 < n_1 \leq 200$ for the $\Delta n = 0$ transitions were estimated by using an $n^{-3}$ extrapolation to the transition rates.

The detailed Auger and electric-dipole radiative rates for each autoionizing state were computed according to Eqs. (3) and (4), respectively. These atomic data were then used to calculate the DR rate coefficients according to Eqs. (1) and (2). The effect of relativity on the DR coefficients from the $\Delta n=0$ transitions is also studied for the $Mo^{33+}$ ion by comparing the relativistic and nonrelativistic Hartree-Fock calculations from the present work.

## IV. RESULTS AND DISCUSSION

Dielectronic-recombination coefficients for the F-like ions were calculated for the six ions with $Z=26$, 35, 42, 47, 54, and 63 using the MCDF model. The calculations cover the electron temperature in the range $0.02 \leq T \leq 9$ keV. The results for the $\Delta n=0$ and $\Delta n \neq 0$ transitions for the three initial states of the recombining ion are listed in Tables I–VI.

The DR rate coefficients from the present MCDF model were evaluated using isolated resonance approximation. For the low-lying $3l3l'$ and $3l4l'$ autoionzing states of the $Fe^{16+}$ ions, the natural linewidths are typically less than 0.3 eV, while the separations between resonances are larger than 0.5 eV. Hence the isolated resonance approximation should be a reasonable approximation for the treatment of the low-lying autoionizing states which con-

TABLE I. Theoretical dielectronic-recombination coefficients (in $10^{-12}$ cm$^3$/sec) for the F-like $_{26}Fe^{17+}$ ion.

| $T$ | $^2S_{1/2}$ | $^2P_{1/2}$ | | $^2P_{3/2}$ | |
|---|---|---|---|---|---|
| (keV) | $\Delta n \neq 0$ | $\Delta n=0$ | $\Delta n \neq 0$ | $\Delta n=0$ | $\Delta n \neq 0$ |
| 0.02 | | 14.2 | | 6.76 | |
| 0.04 | | 13.0 | | 8.65 | |
| 0.06 | | 11.8 | | 8.80 | |
| 0.10 | 6.90 | 8.91 | 7.09 | 7.28 | 6.09 |
| 0.30 | 31.3 | 2.96 | 38.3 | 2.64 | 33.6 |
| 0.50 | 31.5 | 1.54 | 40.4 | 1.40 | 35.6 |
| 0.80 | 24.6 | 0.851 | 32.5 | 0.780 | 28.6 |
| 1.00 | 20.6 | 0.595 | 27.4 | 0.548 | 24.2 |
| 1.50 | 13.8 | 0.334 | 18.6 | 0.309 | 16.5 |
| 2.00 | 9.97 | 0.220 | 13.5 | 0.204 | 12.0 |
| 3.00 | 6.04 | 0.121 | 8.24 | 0.113 | 7.29 |
| 5.00 | 3.06 | 0.057 | 4.19 | 0.053 | 3.71 |
| 7.00 | 1.91 | 0.036 | 2.64 | 0.033 | 2.33 |
| 9.00 | 1.34 | 0.024 | 1.85 | 0.023 | 1.64 |

TABLE II. Theoretical dielectronic-recombination coefficients (in $10^{-12}$ cm$^3$/sec) for the F-like $_{35}Br^{26+}$ ion.

| $T$ | $^2S_{1/2}$ | $^2P_{1/2}$ | | $^2P_{3/2}$ | |
|---|---|---|---|---|---|
| (keV) | $\Delta n \neq 0$ | $\Delta n=0$ | $\Delta n \neq 0$ | $\Delta n=0$ | $\Delta n \neq 0$ |
| 0.02 | | 11.3 | | 11.6 | |
| 0.04 | | 15.4 | | 13.4 | |
| 0.06 | | 16.1 | | 13.3 | |
| 0.10 | 1.55 | 14.5 | 1.35 | 11.8 | 1.10 |
| 0.30 | 23.3 | 5.54 | 24.5 | 5.25 | 20.9 |
| 0.50 | 33.9 | 3.00 | 37.8 | 2.95 | 32.7 |
| 0.80 | 35.2 | 1.69 | 40.8 | 1.70 | 35.6 |
| 1.00 | 32.8 | 1.19 | 38.6 | 1.21 | 33.8 |
| 1.50 | 25.8 | 0.676 | 30.8 | 0.691 | 27.1 |
| 2.00 | 20.2 | 0.448 | 24.4 | 0.460 | 21.5 |
| 3.00 | 13.4 | 0.249 | 16.3 | 0.257 | 14.5 |
| 5.00 | 7.10 | 0.117 | 8.79 | 0.122 | 7.77 |
| 7.00 | 4.59 | 0.074 | 4.77 | 0.077 | 5.04 |
| 9.00 | 3.27 | 0.053 | 3.52 | 0.052 | 3.60 |

TABLE III. Theoretical dielectronic-recombination coefficients (in $10^{-12}$ cm$^3$/sec) for the F-like $Mo^{33+}$ ion.

| $T$ | $^2S_{1/2}$ | $^2P_{1/2}$ | | $^2P_{3/2}$ | |
|---|---|---|---|---|---|
| (keV) | $\Delta n \neq 0$ | $\Delta n=0$ | $\Delta n \neq 0$ | $\Delta n=0$ | $\Delta n \neq 0$ |
| 0.02 | | 14.4 | | 36.1 | |
| 0.04 | | 20.4 | | 29.5 | |
| 0.06 | | 21.8 | | 24.4 | |
| 0.10 | 0.269 | 19.9 | 0.197 | 19.2 | 0.167 |
| 0.30 | 15.1 | 8.60 | 13.8 | 8.92 | 12.5 |
| 0.50 | 27.5 | 4.77 | 26.6 | 5.22 | 24.4 |
| 0.80 | 33.9 | 2.72 | 34.1 | 3.07 | 31.4 |
| 1.00 | 34.2 | 1.93 | 34.8 | 2.22 | 32.1 |
| 1.50 | 30.3 | 1.10 | 31.6 | 1.29 | 29.2 |
| 2.00 | 25.4 | 0.732 | 26.9 | 0.865 | 24.9 |
| 3.00 | 18.2 | 0.408 | 19.4 | 0.487 | 17.9 |
| 5.00 | 10.6 | 0.193 | 11.3 | 0.232 | 10.5 |
| 7.00 | 7.02 | 0.122 | 7.58 | 0.147 | 7.03 |
| 9.00 | 5.09 | 0.083 | 5.50 | 0.100 | 5.10 |

TABLE IV. Theoretical dielectronic-recombination coefficients (in $10^{-12}$ cm$^3$/sec) for the F-like $Ag^{38+}$ ion.

| $T$ (keV) | $^2S_{1/2}$ $\Delta n\neq 0$ | $^2P_{1/2}$ $\Delta n=0$ | $^2P_{1/2}$ $\Delta n\neq 0$ | $^2P_{3/2}$ $\Delta n=0$ | $^2P_{3/2}$ $\Delta n\neq 0$ |
|---|---|---|---|---|---|
| 0.02 | | 74.6 | | 40.7 | |
| 0.04 | | 48.8 | | 36.7 | |
| 0.06 | | 40.2 | | 30.2 | |
| 0.10 | 0.060 | 31.3 | 0.040 | 23.3 | 0.032 |
| 0.30 | 9.71 | 12.6 | 8.51 | 11.6 | 7.51 |
| 0.50 | 21.4 | 6.96 | 19.8 | 7.09 | 17.9 |
| 0.80 | 29.3 | 3.97 | 28.2 | 4.30 | 25.9 |
| 1.00 | 30.8 | 2.82 | 30.2 | 3.16 | 27.8 |
| 1.50 | 29.4 | 1.61 | 29.6 | 1.86 | 27.4 |
| 2.00 | 25.9 | 1.07 | 26.4 | 1.26 | 24.6 |
| 3.00 | 19.5 | 0.597 | 20.2 | 0.714 | 18.7 |
| 5.00 | 11.7 | 0.283 | 12.3 | 0.343 | 11.4 |
| 7.00 | 7.96 | 0.179 | 8.40 | 0.218 | 7.81 |
| 9.00 | 5.85 | 0.121 | 6.18 | 0.149 | 5.75 |

TABLE V. Theoretical dielectronic-recombination coefficients (in $10^{-12}$ cm$^3$/sec) for the F-like $Xe^{45+}$ ion.

| $T$ (keV) | $^2S_{1/2}$ $\Delta n\neq 0$ | $^2P_{1/2}$ $\Delta n=0$ | $^2P_{1/2}$ $\Delta n\neq 0$ | $^2P_{3/2}$ $\Delta n=0$ | $^2P_{3/2}$ $\Delta n\neq 0$ |
|---|---|---|---|---|---|
| 0.02 | | 47.5 | | 8.16 | |
| 0.04 | | 47.0 | | 20.7 | |
| 0.06 | | 43.5 | | 23.3 | |
| 0.10 | 0.0074 | 36.9 | 0.0043 | 22.2 | 0.0027 |
| 0.30 | 4.08 | 16.4 | 3.99 | 14.3 | 3.01 |
| 0.50 | 12.6 | 9.32 | 12.8 | 9.72 | 10.2 |
| 0.80 | 20.6 | 5.38 | 21.3 | 6.27 | 17.5 |
| 1.00 | 23.2 | 3.85 | 23.8 | 4.74 | 20.0 |
| 1.50 | 24.6 | 2.21 | 25.3 | 2.90 | 21.6 |
| 2.00 | 23.2 | 1.48 | 23.8 | 2.00 | 20.6 |
| 3.00 | 18.8 | 0.826 | 19.4 | 1.15 | 17.1 |
| 5.00 | 12.4 | 0.392 | 12.8 | 0.562 | 11.4 |
| 7.00 | 8.74 | 0.248 | 8.98 | 0.360 | 8.07 |
| 9.00 | 6.55 | 0.169 | 6.74 | 0.246 | 6.07 |

TABLE VI. Theoretical dielectronic-recombination coefficients (in $10^{-12}$ cm$^3$/sec) for the F-like $Eu^{54+}$ ion.

| $T$ (keV) | $^2S_{1/2}$ $\Delta n\neq 0$ | $^2P_{1/2}$ $\Delta n=0$ | $^2P_{1/2}$ $\Delta n\neq 0$ | $^2P_{3/2}$ $\Delta n=0$ | $^2P_{3/2}$ $\Delta n\neq 0$ |
|---|---|---|---|---|---|
| 0.02 | | 26.1 | | 0.0058 | |
| 0.04 | | 40.2 | | 0.693 | |
| 0.06 | | 42.0 | | 2.77 | |
| 0.10 | 0.0060 | 39.0 | 0.0004 | 6.92 | 0.0002 |
| 0.30 | 1.21 | 19.5 | 0.974 | 11.5 | 0.779 |
| 0.50 | 6.10 | 11.4 | 5.18 | 9.94 | 4.39 |
| 0.80 | 12.9 | 6.71 | 11.3 | 7.40 | 10.1 |
| 1.00 | 15.8 | 4.84 | 14.0 | 6.01 | 12.7 |
| 1.50 | 19.0 | 2.80 | 17.4 | 3.97 | 15.9 |
| 2.00 | 19.3 | 1.88 | 18.0 | 2.85 | 16.6 |
| 3.00 | 17.4 | 1.05 | 16.6 | 1.72 | 15.3 |
| 5.00 | 12.6 | 0.503 | 12.3 | 0.867 | 11.3 |
| 7.00 | 9.34 | 0.319 | 9.14 | 0.562 | 8.42 |
| 9.00 | 7.20 | 0.217 | 7.08 | 0.388 | 6.52 |

tribute the most to the total DR coefficients except for the low-temperature region.

In the present work, we include all the possible Auger decay channels and radiative channels leading to the stabilized bound states. The radiative transitions to the other autoionizing states were neglected both in $A_r$ and $\Gamma_r$ of Eq. (2) (i.e., the truncated approximation).[21] For the Ne-like and He-like ions, the DR coefficients from this truncated approximation have been found to agree with the values obtained by including full radiative cascade effect to within 3%.[7,21] Therefore we expect the truncated approximation used in the present calculations to yield reasonable good results.

For the $\Delta n=0$ transitions, we include the contribution from the autoionizing states with angular momentum $l_1 \leq 8$ [see Eq. (6)]. The contribution to the DR coefficient by the autoionizing states with angular momentum $8 < l_1 \leq 15$ has been found to be only a few percent for the fluorine isoelectronic sequence.[22]

The partial DR rate coefficients from the $3lnl'$ configurations for $Z=26$ and 42 are compared in Fig. 1. At the peak temperature, the DR coefficient is dominated by the contributions from $n \leq 6$ configurations. For higher temperature, high $n$ becomes increasingly important. Furthermore, the DR coefficient converges much faster for the heavy ion than for the light ion.

In Fig. 2 we compare the DR rate coefficients from our present relativistic and nonrelativistic Hartree-Fock calculations for the $\Delta n=0$ transitions in the $Mo^{33+}$ ion.

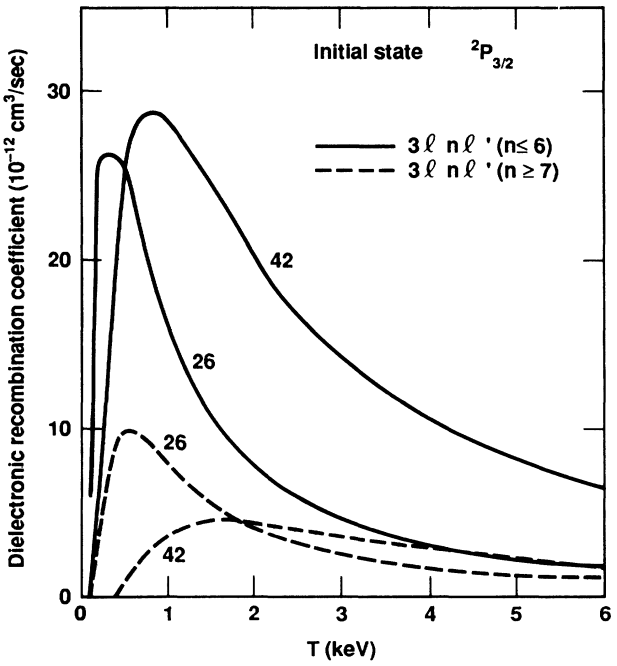


FIG. 1. Partial dielectronic rate coefficients for the initial $^2P_{3/2}$ state as functions of electron temperature. The numbers labeling the curves are the atomic numbers of the ions. The solid curves represent the contributions from the intermediate $3lnl'$ states with $n \leq 6$, while the dashed curves indicate the results for $n \geq 7$.

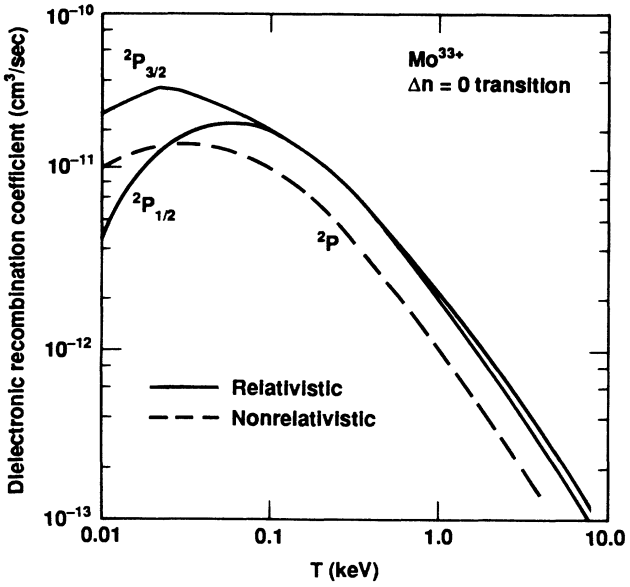


FIG. 2. Dielectronic rate coefficients for the $\Delta n=0$ transitions of the $Mo^{33+}$ as functions of temperature. The solid curves display the results from the relativistic calculations. The dashed curve shows the nonrelativistic predictions.

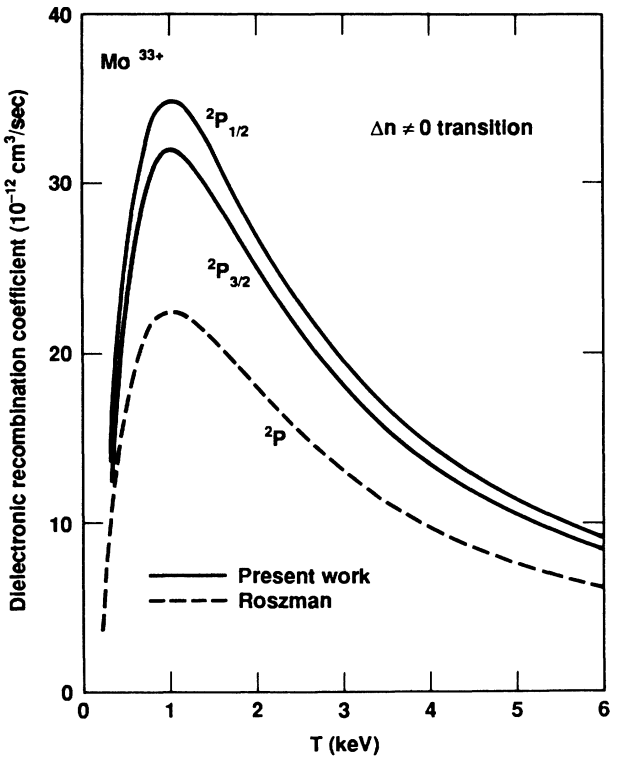


FIG. 4. Same as Fig. 3 except using the $Mo^{33+}$ ion.

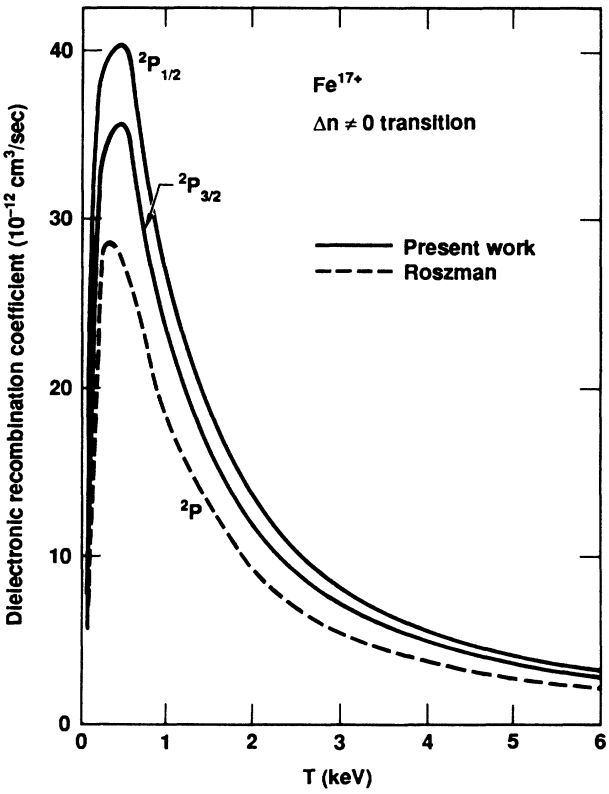


FIG. 3. Dielectronic rate coefficients for the $\Delta n\neq 0$ transitions of the $Fe^{17+}$ ion a functions of temperature. The solid curves represent the present MCDF results. The dashed curve indicates the values from the Hartree-Fock calculations of Ref. 14.

The relativistic results are larger than the predictions from the nonrelativistic model by a factor of 2. This enhancement is mainly due to the increase in the $2s$-$2p$ radiative rates because of the relativistic effect on the $2s$-$2p$ transition energies.

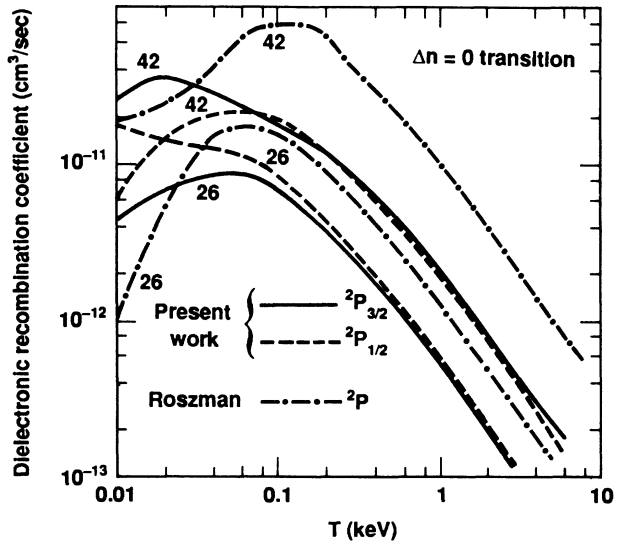


FIG. 5. Dielectronic rate coefficients for the $\Delta n=0$ transitions as functions of temperature. The solid and dashed curves show the results from the present MCDF model for the initial $^2P_{3/2}$ and $^2P_{1/2}$ states, respectively. The dot-dashed curve represents the values from Ref. 14. The numbers labeling the curves are the atomic numbers of the ions.

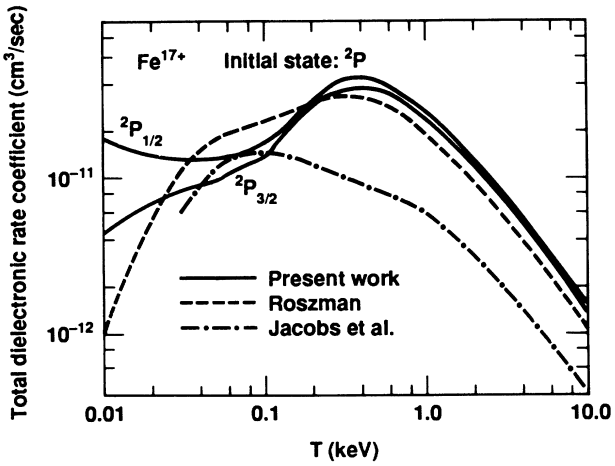


FIG. 6. Total dielectronic rate coefficients for the initial $^2P$ states of the $Fe^{17+}$ ion as functions of temperature. The solid curves display the predictions from the present MCDF model. The dashed curve indicates the results from the HF calculations (Ref. 14) and the dot-dashed curve represents the theoretical values from Jacobs *et al.* (Ref. 11).

The dielectronic recombination for the F-like ions has previously been investigated for several ions by Roszman[14] using the distorted-wave method. The detailed Auger and radiative rates were calculated using nonrelativistic single-configuration Hartree-Fock wave functions (HF) in *LS* coupling. The theoretical predictions from our present MCDF model are compared with the results from Roszman's Hartree-Fock calculations in Figs. 3–7. For the $\Delta n \neq 0$ transitions of the $Fe^{17+}$ ion, the MCDF values are larger than the HF results by $\sim 20\%$ (Fig. 3). This deviation is probably caused by the relativistic effect. The DR rate coefficient for the $^2P_{1/2}$ state is larger than the rate for the $^2P_{3/2}$ state by an amount of 15% at the peak value due to the inclusion of the spin-orbit interaction in the present calculations. For the $Mo^{33+}$ ion, the present MCDF results are larger than the HF predictions by a factor of 1.5 (see Fig. 4).

The dielectronic-recombination coefficients from the $\Delta n = 0$ transitions for the $Fe^{17+}$ and $Mo^{33+}$ ions are compared in Fig. 5. The rate coefficient typically peaks at low temperature. The DR coefficients for the $^2P_{1/2}$ and $^2P_{3/2}$ states are quite different at very low temperatures because the DR rate coefficients are very sensitive to the Auger energies for such low temperatures. The predictions from the HF calculations[14] have been found to differ from the present MCDF results by as much as a factor of 4. This is partly due to the sensitivity of the Coster-Kronig rates on the differences in the atomic models.

In Fig. 6 the total DR rate coefficients for the $Fe^{17+}$ ion from the present work are compared with the previous theoretical results. The total DR rate coefficients show a two-hump structure because the $\Delta n = 0$ and $\Delta n \neq 0$ transitions peak at different temperatures. For electron temperatures $30 \leq T \leq 100$ eV, our present results agree with those of Jacobs *et al.*,[11] but differ from

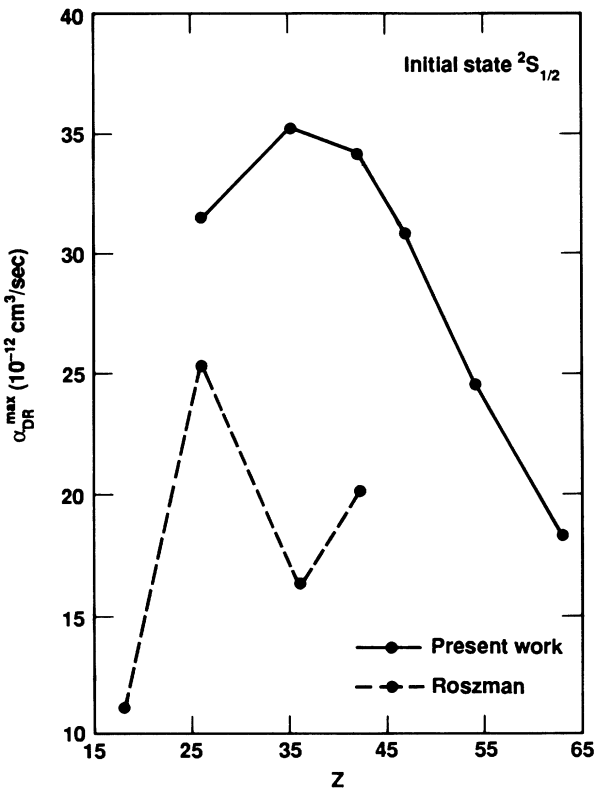


FIG. 7. Maximum dielectronic rate coefficients for the initial $^2S_{1/2}$ state as functions of atomic number. The solid curve indicates the present results and the dashed curve shows the HF predictions from Ref. 14. The lines were drawn to guide the eyes.

Roszman's value by as much as 60%. This implies that the rates for the $\Delta n = 0$ transitions from the present work agree quite well with the predictions based on the quantum-defect extrapolation.[11] For the temperature $T > 100$ eV, however, the present MCDF results agree with the HF values of Roszman to within 30%. The results from Jacobs *et al.*[11] are smaller by a factor of 5 due to the inappropriate treatment of the Auger transitions to the excited states.[23]

The maximum dielectronic rate coefficients $\alpha_{DR}^{max}$ for the $^2S_{1/2}$ state are displayed in Fig. 7. The $\alpha_{DR}^{max}$ from the present calculations peaks around $Z = 36$, while the results from Ref. 14 show a strong dip instead at $Z = 36$. This strange behavior of the HF calculations from Ref. 14 has recently been found due to the numerical errors in the basis set expansion for $Z \geq 36$.[22] The large discrepancies between the present work and the values given in Ref. 14 for the ions with $Z \geq 36$ can mostly be attributed to the numerical errors in Ref. 14.

## ACKNOWLEDGMENT

This work was performed under the auspices of the U.S. Department of Energy by the Lawrence Livermore National Laboratory under Contract No. W-7405-ENG-48.

[1]A. Burgess, Astrophys. J. **139**, 776 (1964); **141**, 1589 (1965).
[2]M. J. Seaton and P. J. Storey, in *Atomic Processes and Applications,* edited by P. G. Burke and B. L. Moiseiwitsch (North-Holland, Amsterdam, 1976), p. 133.
[3]J. Dubau and S. Volonte, Rep. Prog. Phys. **43**, 199 (1980).
[4]H. P. Summers, Mon. Not. R. Astron. Soc. **169**, 663 (1974).
[5]B. L. Whitten, A. U. Hazi, M. H. Chen, and P. L. Hagelstein, Phys. Rev. A **33**, 2171 (1986).
[6]A. L. Merts, R. D. Cowan, and N. H. Magee, Jr., Los Alamos Scientific Laboratory Report No. LA-6220-MS, 1976 (unpublished).
[7]M. H. Chen, Phys. Rev A **33**, 994 (1986); **34**, 1073 (1986).
[8]L. J. Roszman, Phys. Rev. A **20**, 673 (1979); **35**, 2122 (1987).
[9]K. LaGattuta and Y. Hahn, Phys. Rev. A **27**, 1675 (1983); Phys. Rev. Lett. **51**, 558 (1983).
[10]D. C. Griffin, M. S. Pindzola, and C. Bottcher, Phys. Rev. A **31**, 568 (1985).
[11]V. L. Jacobs, J. Davis, P. C. Kepple, and M. Blaha, Astrophys. J. **211**, 605 (1977).
[12]S. Dalhed, J. Nilsen, and P. Hagelstein, Phys. Rev. A **33**, 264 (1986).
[13]C. P. Bhalla and K. R. Karim, Phys. Rev. A **34**, 3525 (1986); **34**, 4743 (1986).
[14]L. J. Roszman, Phys. Rev. A **35**, 2138 (1987).
[15]P. L. Hagelstein, J. Phys. B **20**, 5785 (1987).
[16]M. H. Chen, Phys. Rev. A **34**, 1079 (1986).
[17]M. H. Chen, Phys. Rev. A **31**, 1449 (1985).
[18]I. P. Grant, B. J. McKenzie, P. H. Norington, D. F. Mayers, and N. C. Pyper, Comput. Phys. Commun. **21**, 207 (1980).
[19]W. Bambynek, B. Crasemann, R. W. Fink, H. U. Freund, H. Mark, C. D. Swift, R. E. Price, and P. V. Rao, Rev. Mod. Phys. **44**, 716 (1972).
[20]I. P. Grant, J. Phys. B **7**, 1458 (1974).
[21]J. N. Gau, Y. Hahn, and J. A. Retter, J. Quant. Spectrosc. Radiat. Transfer **23**, 147 (1979).
[22]L. J. Roszman (private communication).
[23]P. L. Hagelstein, M. D. Rosen, and V. L. Jacobs, Phys. Rev. A **34**, 1931 (1986).